



Devising a novel method of producing high transparent magnesium aluminate spinel ($MgAl_2O_4$) ceramics body using synthesized LiF nanopowder and spark plasma sintering

Masoud Azizi-Malekabadi, Rasoul Sarraf-Mamoory^{*}

Materials Department, Faculty of Engineering, Tarbiat Modares University, Tehran, Iran

HIGHLIGHTS

- The transmission of the sample achieved 86.8% at the wavelength of 1100 nm.
- The ready-to-sinter spinel led to a decrease in sintering temperature to 1100 °C.
- The final strength of the sintered sample obtained 97.8 MPa.
- The density of the sintered sample obtained 99.98%.
- The ready-to-sinter spinel method is easier than other chemical synthesis methods.

ARTICLE INFO

Keywords:

Spinel $MgAl_2O_4$
LiF
Transparent ceramics
Spark plasma sintering
Sintering aid

ABSTRACT

In this study, to achieve high transparency of magnesium aluminate spinel, the ready-to-sinter spinel (RSS) powder was sintered by spark plasma sintering (SPS). To prepare the RSS powder, LiF nanopowder was synthesized at diverse temperatures and concentrations on the spinel powder surface (0.7 wt %). The optimal temperature and concentration were achieved to be (60 °C) and (200 g/l), respectively. Then, the spinel body was fabricated by SPS method. The XRD, BET, ICP, FESEM and TEM analyses were applied for the characterization of the prepared powder. Also, the results of TEM and XRD analysis confirmed the presence of the fluoride light element (LiF compound) on the spinel particles surface. Finally, the final strength and density of the spinel body were measured 97.8 MPa and 99.98% respectively, with the transmission of 86.8% at the wavelength of 1100 nm after sintering at 1100 °C.

1. Introduction

The $MgAl_2O_4$ spinel has great importance in modern technologies, because of its interesting properties [1–10]. It has an acceptable thermal shock resistance, significant mechanical strength, and high melting point (2135 °C), and low thermal expansion coefficient [11–17]. It also has an acceptable toughness and high hardness [18,19]. The $MgAl_2O_4$ spinel as a kind of optical materials has a broad range of applications in different engineering parts, including the medical application (implants, anti-wear coatings), optical lenses, smartphones (anti-wear and shock-proof plates), watches (anti-wear and anti-shock lenses with high strength), cars, and etc [20–23]. The principal aim in the development of $MgAl_2O_4$ spinel ceramics is to achieve optical transparency and suitable mechanical properties. The developments in different sectors such as

powder synthesis, shaping and sintering can make achievable fabricating of high transparent spinel ceramic. Generally, high-quality initial nanopowder, suitable powder pre-treatment, sintering aids, and sintering processes are vital factors to obtain transparent spinel ceramics [24].

Lithium fluoride is widely used as an additive material serving as a sintering aid and as a component for high capacity electrode materials used in Li-ion batteries [25,26]. Moreover, the physical methods used to synthesize metal fluorides, such as mechanical milling, laser dispersion or molecular-beam epitaxy, some chemical methods like hydrothermal treatment, micro emulsion, precipitation, mechano-chemical method, and the sol-gel method should also be noted [27,28]. Spinel is known to be densified by the sintering aids; this is such that many materials such as $CaCO_3$, CaO , B_2O_3 , $AlCl_3$, AlF_3 , Na_3AlF_6 and LiF has been recommended for powder densification [29,30]. However, the only material

^{*} Corresponding author.

E-mail address: rsarrafm@modares.ac.ir (R. Sarraf-Mamoory).

Table 1

RSS powder synthesis under different concentrations and temperatures of the LiOH solution.

RSS Powder Sample	LiOH Solution Concentration (g/l)	LiOH Solution Temperature (°C)
a	20 (Low)	4 (Low)
b	200 (High)	4 (Low)
c	200 (High)	60 (High)

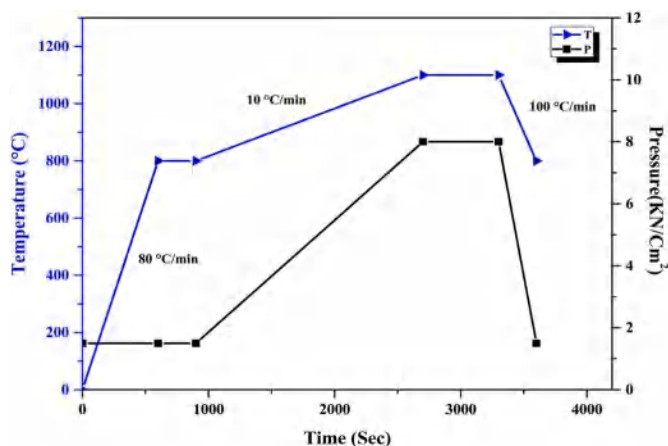


Fig. 1. The SPS cycle.

producing the least number with the homogenous porosity and contamination in the sintered spinel is lithium fluoride [30–39]. So, owing to possess the maximum effect of additive (without the decrease of mechanical and optical properties in the final product), raw materials and additives should be distributed homogeneously. Transparent MgAl_2O_4 are usually sintered by hot press (HP), hot isostatic press (HIP) and spark plasma sintering (SPS) methods. The SPS method can be used to consolidate ceramic powders to fully dense parts during a short time at low temperatures which can make maximum densification and limited grain growth [40]. Frage et al. have reported the conditions for the fabrication of transparent spinel using the SPS method with LiF (1 wt %) as a sintering aid [30]. The highest transparency of the product in the visual wavelength range was about 75%. Morita et al. have achieved the results of transparent spinel fabrication also by SPS at 1300 °C without additives, and the transparency which was obtained 55% [41]. Zegadi et al. have sintered commercial powders by SPS between 1250 and 1350

°C with an incremental step of 20 °C and after sintering at $T = 1350$ °C exhibits the highest real in line transmission (83.6%) at the wavelength of 550 nm which was enhanced by a post-annealing at 1200 °C up to ~ 85% [42].

In this study, a fully dense MgAl_2O_4 spinel body was fabricated with high transparency, and the LiF nano powder was uniformly synthesized on the surface of the spinel powder as a sintering aid. Furthermore, the presence of LiF nanoparticles (0.7 wt %) led to the decrease of the spinel sintering temperature to 1100 °C. Finally, the final strength, density, and transmission at the 1100 nm wavelength of the spinel body were obtained 97.8 MPa, 99.98%, and 86.8%, respectively after SPS at 1100 °C.

2. Materials and methods

In this study, highly pure powder of spinel was synthesized via highly pure powder of $\alpha\text{-Al}_2\text{O}_3$, and the highly pure powder of magnesia [43]. The synthesized spinel powder, Ethanol (99.6%, Merck, Germany), Extra pure acetone (>99%, Merck, Germany), Lithium hydroxide (99.9%, Merck, Germany), Hydrofluoric acid (60%, Merck, Germany), and de-ionized water (18 M Ω) were used as precursors.

LiF nano powder was synthesized on the spinel particle surface by chemically in-situ method, and the effect of concentration and temperature of lithium hydroxide solution on the size of LiF nano-particles was studied [27,43]. For this purpose, lithium hydroxide solutions were prepared by 100 cc de-ionized water (20 g/l and 200 g/l concentrations) according to Table 1, and the spinel powder was mixed with them, separately. Then, the mixed powder was deagglomerated by the ultrasonic probe (20 KH, 400 W, Topsonic, Iran) during 30 S and with 100 W energy. Hydrofluoric acid was added to the suspensions during stirring at 4 and 60 °C, separately. Afterwards, 200 cc acetone was instantly poured into the suspensions. After suspensions mixing for 10 min, they were poured on filter paper, and washed by de-ionized water three times so as to remove the impurities. Eventually, the final powder ready-to-sinter spinel (RSS) was put in the oven at 50 °C. The RSS powder was sintered by SPS method at 1100 °C under 8 kN/Cm² pressure, for 60 min with the heating rate of 10 °C/min by SPS-1050 (SPS Syntex Inc., Kawasaki, Japan) under vacuum 10^{-4} bar utilizing graphite

Table 2

Chemical analysis (ICP) of the synthesized spinel powder.

Element (ppm)	Ca	Fe	K	Li	Na	S
Spinel Powder	115	70	121	258	339	18

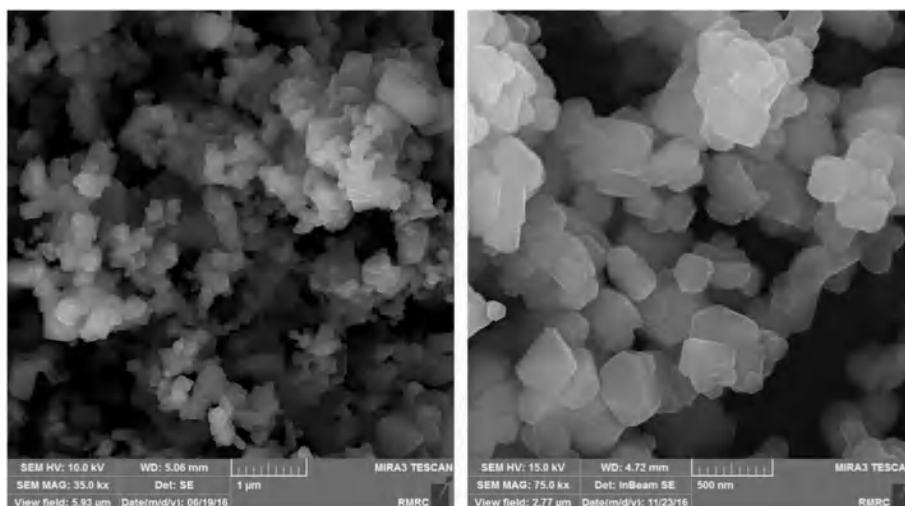


Fig. 2. FESEM image of the synthesized spinel powder.

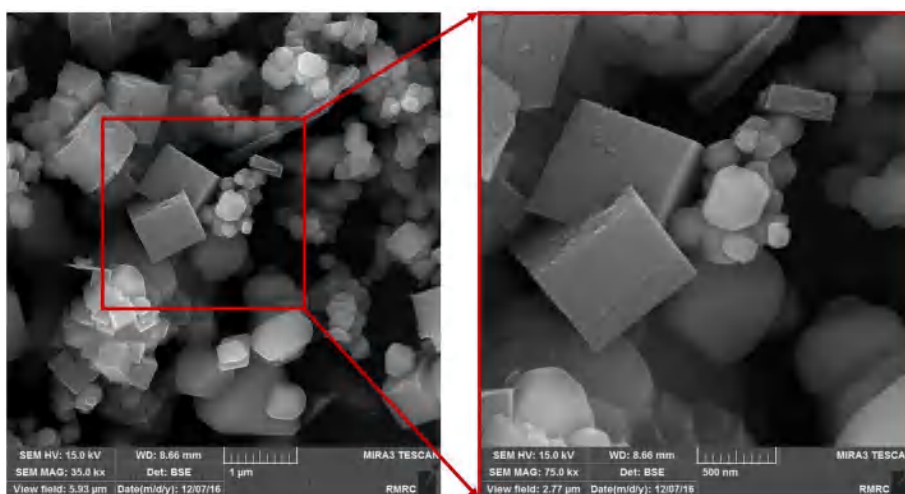


Fig. 3. FESEM images (RSS powder of sample a) at 4 °C and 20 g/l LiOH.

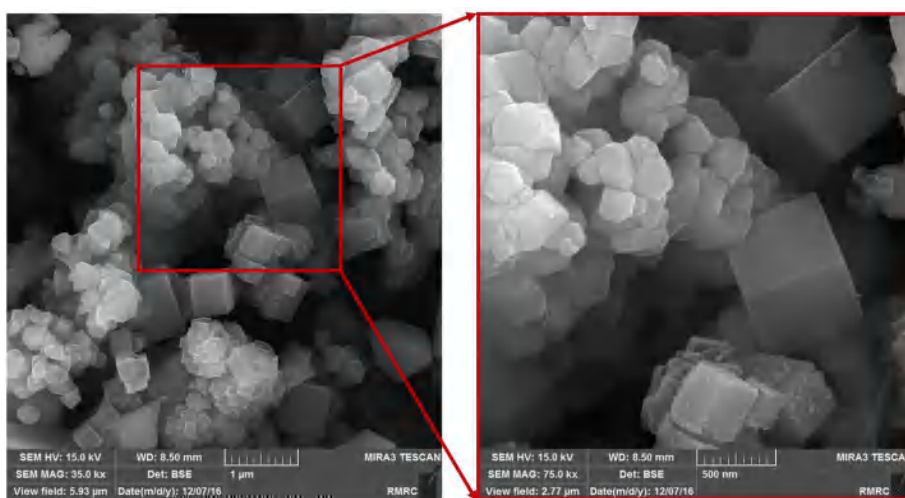


Fig. 4. FESEM images (RSS powder of sample b) at 4 °C and 200 g/l LiOH.

die with a 20 mm inner diameter. Fig. 1 shows the SPS cycle of sintered RSS powder. Briefly, the flowchart of spinel body preparation is shown in Supplemental Fig. 1 (Appendix A. Supplementary data).

The inductively coupled plasma-optical emission spectrometer (ICP-OES) (Optima-4300DV, PerkinElmer Inc., MA, and the USA) was used to determine the purity of the powder. Measurement of the specific surface area of the powders was done by utilizing the BET (Micromeritics instrument corporation, Japan) method by nitrogen adsorption. A Philips X'PERT MPD X-ray diffractometer with CuK α Radiation (λ CuK α 1 = 0.154 nm, incident angle = 0.03°) was utilized to characterize the powder samples. The investigation of the powder particles morphology and the microstructure of the spinel body after sintering was carried out by a field emission scanning electron microscopy (FESEM, Mira 3-XMU) and energy-dispersive X-ray spectroscopy (EDS). Transmission electron microscopy (TEM) with high-angle annular dark-field detector (HAADF) analysis was also conducted using FEI Titan Themis. In order to measure the optical transmittance of the MgAl₂O₄ spinel body, a UV-visible spectrophotometer (Model U-2800, Hitachi, Tokyo, Japan) was utilized. The wavelength was studied in the range of 200–1100 nm. The spinel body samples strength were measured by the three-point bending test (H50KS, Hounsfield, England). The cylindrical shape samples 18.17 mm diameter and thickness of 2.210 mm were located under the jaws of the three-point bending test, and their strength was studied.

3. Results and discussion

Fig. 2 shows the spinel powder with semi-spherical morphology and the average size 100 nm. The ICP results of the high pure spinel powder are shown in Table 2. Sintering aids are added to the spinel powder by mixing (random) or colloidal (regular) processing. Colloidal processing is more complex than mixing, since it needs chemical processing, heat treatment, and crashing. As a result of the regular mixing of the spinel powder and the LiF sintering aid, the formation of a heterogeneous region during sintering that would decrease the mechanical and optical properties could be avoided [44]. For the effective sintering of the spinel powder, a low amount of LiF sintering aid particles should be used. Loutfy et al. worked on the induced precipitation mixing method for nano-mixing magnesium aluminate spinel with a uniformly distributed which consisted of LiF sintering aid to make the ready-to-sinter spinel (RSS) powder [45].

The RSS powder was synthesized by 0.7 wt% nano LiF sintering aid in different temperatures and concentrations, and addition of acetone. According to sample a in Fig. 3, there are a few of large LiF particles beside spinel particles due to very few places for nucleation. Also, the formed crystals were grown by transferring the materials from ion rich regions to the poor ones. Moreover, in the low temperature due to the lower nucleation rate, the few LiF particles were synthesized [46]. Fig. 4

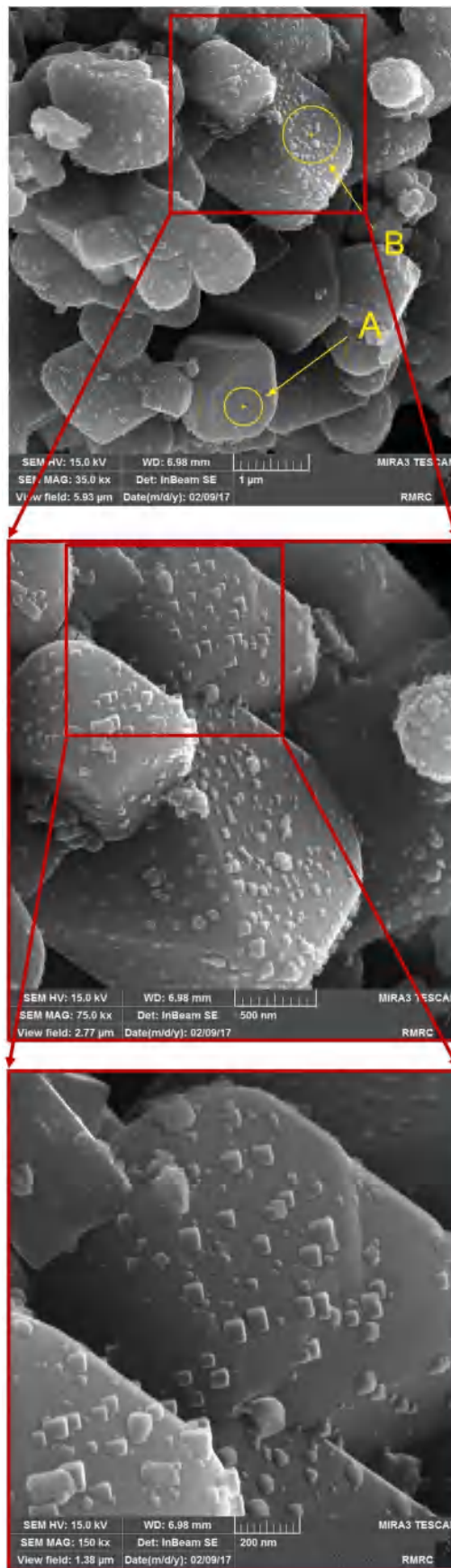


Fig. 5. FESEM images (RSS powder of sample c) at 60 °C and 200 g/l LiOH.

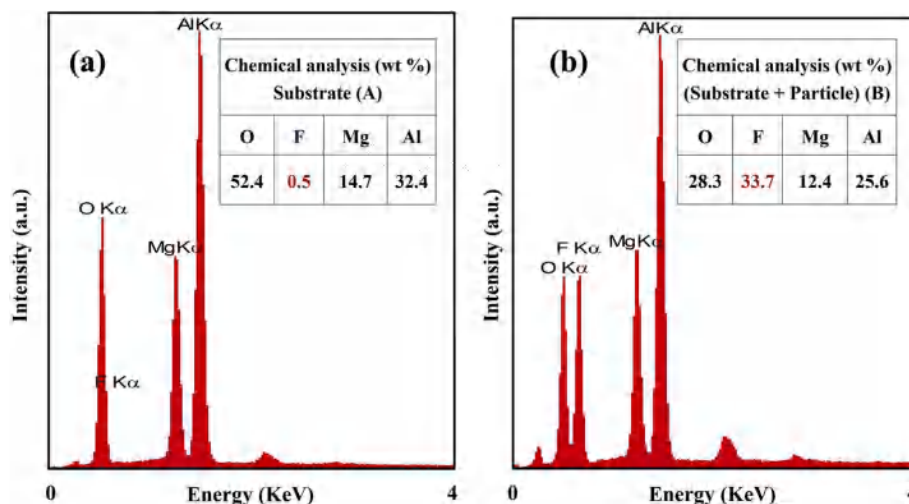


Fig. 6. Results of EDS quantity analysis from (a) A point, and (b) B point.

shows a reduction in LiF particles size of sample b due to the concentration increase of LiOH solution at constant temperature compared to sample a. Fig. 5 shows some of the cubic LiF nanoparticles on the spinel substrate homogeneously at higher temperature and constant concentration compared to sample b. In fact, nucleation process would dominate the growth process, and the number of nuclei was increased in the sample c. The effect of temperature on heterogeneous nucleation was calculated by equation (1):

$$J_{\text{het}} = \Omega_{\text{het}} \exp(-\Delta G_{\text{het}}^* / kT) \quad (1)$$

Equation (1) shows the heterogeneous nucleation rate. Where J is the nucleation rate, ΔG is the free energy of the system, $k = 1.38 \times 10^{23}$ J/K, T is temperature, and $\Omega = 2D/d^2$ (D is the diffusion coefficient, and d is the interlaminar spacing between the crystal surfaces) [46]. The appropriate distribution of LiF nanoparticles on the surface of spinel particles was homogeneously occurred, that improved the sintering properties. According to Fig. 6, the results of EDS quantity analysis showed pure spinel (point A) and cubic LiF/spinel nanoparticles (point B) and the higher weight percentage of fluoride in the point B (33.7 wt %) as compared to the point A (0.5 wt%), confirming the presence of LiF nanoparticles on the spinel substrate. Fig. 7(a) shows LiF nanoparticles, which were brighter than the spinel substrate. Also, Fig. 7(c) confirmed the presence of LiF composition on spinel surface. Fig. 8 shows the X-ray diffraction patterns of synthesized powder samples ((I) LiF, (II) spinel, and (III) spinel with 20 wt% nano LiF). It should be noted that 20 wt% LiF was coated in the spinel powder surface in order to confirm its phase by X-ray analysis. According to the data below, intensity of sample II peaks were measured in 60, 56, and 78 angles so as to compare to sample III for identifying LiF phase.

Sample II		Sample III		
I_{400}/I_{511}	<	I_{400}/I_{511}	→	$1.26 < 1.43$
I_{400}/I_{422}	<	I_{400}/I_{422}	→	$5.93 < 6.47$
I_{400}/I_{533}	<	I_{400}/I_{533}	→	$5.43 < 6.22$

Hence, the presence of the LiF phase was proven in sample (III). Also, no impurities were detected in the sample (III) during synthesis of LiF nanoparticles on spinel surface. Fig. 9 shows the cubic morphology of coated LiF nanoparticles on spinel powder surface. There are two problems during adding the LiF additive to spinel powder and preparing the RSS powder. The first problem is the heterogeneous distribution of the additive, and the second problem is contamination by mechanical mixing methods. To solve the contamination problem, Villalobos et al. formed a 1 wt% LiF coating on spinel particles, and used spray drying to get more a homogeneous distribution of the LiF on the spinel powder.

There are some disadvantages including low productivity (68%), possible contamination during spray-drying resulting from solution pumping, dryer heater, hot air pollution, and the contact with the metallic components of the spray dryer, declining the commercial application of this method [45]. Sanghera et al. prepared the RSS powder by mixing magnesium aluminate core and fluoride salt solution in a solvent, and the obtained slurry was sprayed in a dry column with oxide atmosphere at the temperature range of 400–750 °C [47–49]. The powder synthesis method of present study was better than costly methods such as fluidized bed, drying column and spray-drying. It was independent of different parameters including special atmosphere (oxide), separation conditions, drying, and deagglomeration unlike the fluidized bed method. Also, the problems of possible contamination in the final powder, the high cost equipment, and energy-wasting were tackled using glass and plastic equipment and low temperatures processing (maximum 60 °C) of the present method as compared to the spray-drying method. Furthermore, its efficiency was increased from 68 to 95%, and the final powder did not need calcination to remove the organic compounds [45,48–52]. The RSS method was used for other engineering ceramics [50,53]. According to Fig. 10, it seems that the minor charges of acetone chains created LiF solvation which prevented the growth of LiF nanoparticles. The minor charge of oxygen in acetone structure was more negative and stronger than oxygen minor charge in water structure. Meanwhile, regard to hard & soft acids and bases theory (HSAB theory), hard acid (Li^+) was more inclined to the solvation. Acetone big molecules occupied around Li^+ ion, preventing from ionic bonding with F^- ion and LiF formation, so that Li^+ solvation would dominate LiF high ionic bond strength. The acetone played a preventive role to inhibit the uncontrolled growth and agglomeration of LiF particles [46]. After preparation of powder, the RSS powder was sintered by SPS. Platinum sheets were utilized for decreasing carbon diffusion, and enhancing transmission in the spinel body. The SPS technique has some benefits including the short sintering time and the ability to achieve dense and transparent optical ceramics [47]. In this research, spinel ceramic body was made by the synthesis of RSS powder, which sintered at 1100 °C by a heating rate of 10 °C/min and the pressure of 8 kN/Cm² for 60 min. The in-line transmittance was achieved 86.8% at the wavelength of 1100 nm with a thickness of 2.210 mm. Ping Fu et al. realized that the optimal annealing temperature (900 °C) reduced carbon and oxygen vacancies. If the annealing temperature was raised to more than 1000 °C, oxygen vacancies and pores would result in a decrease in transparency. Ping Fu et al. could achieve the in-line transmittance of 74.9% at the wavelength of 550 nm [54]. Benaissa et al. sintered nano spinel powder at 1300 °C, 1350 °C and 1400 °C by the SPS method, and obtained ultimate densities of 99.93%, 99.63% and

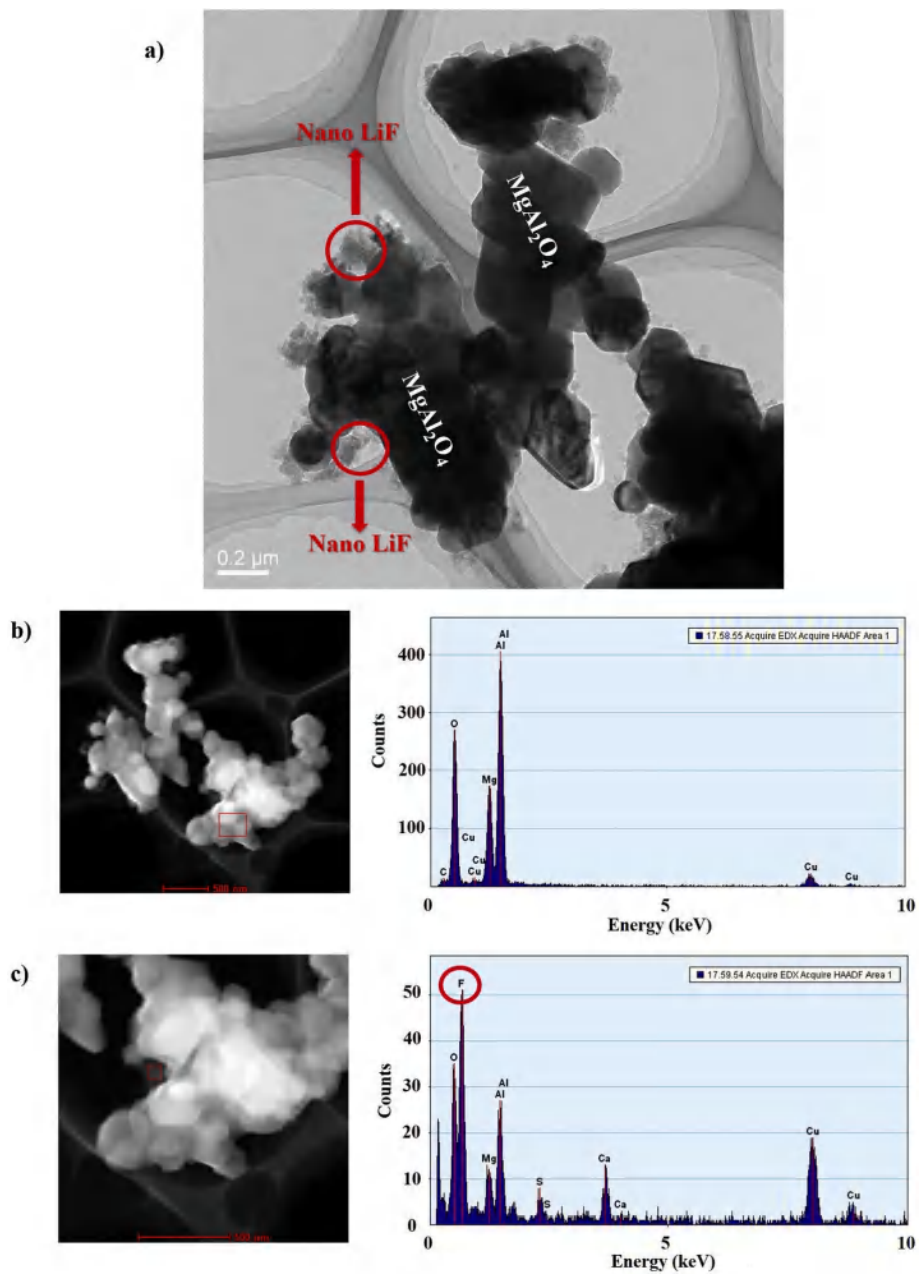


Fig. 7. TEM images of (a) bright field, and area HAADF of the (b) substrate, (c) nanoparticles on the substrate surface.

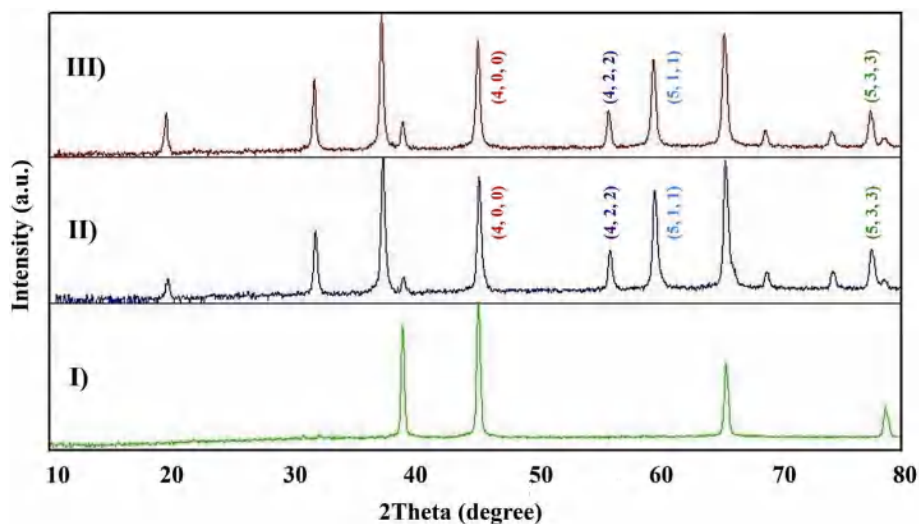


Fig. 8. X ray diffraction patterns of (a) LiF (b) spinel, and (c) spinel powder with 20 wt% LiF.

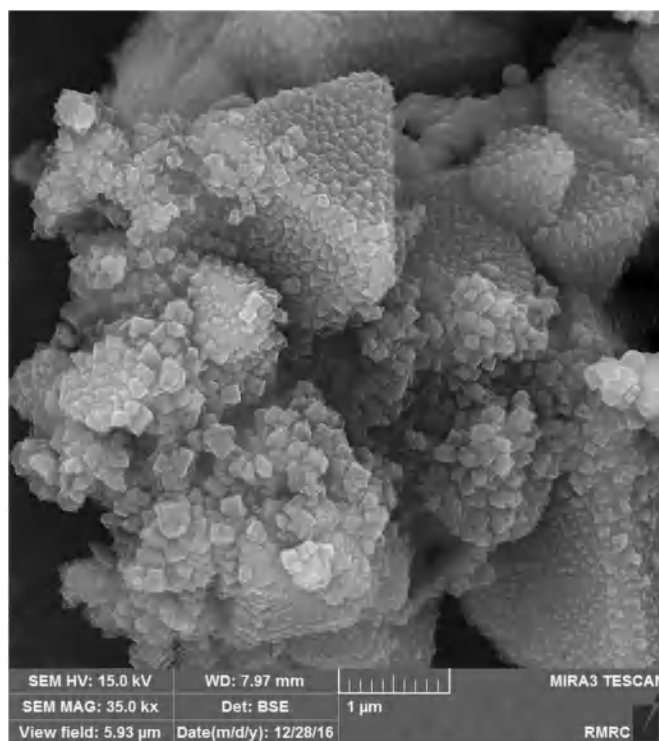


Fig. 9. FESEM image of coated LiF nanoparticles (20 wt %) on spinel powder surface.

99.58%, respectively. Also, they obtained the in-line transmittance at 1300 °C was 78% in wavelength of 1100 nm [55]. Fig. 11 indicates the in-line transmittance diagram of the SPS-sintered RSS powder. As can be seen in Fig. 12, the sintered body was created the structure of dense and pore-free, leading to a shortage of refraction, and the increase in the in-line transmittance. The relative density and strength of the sintered body were obtained 99.98% and 97.8 MPa.

4. Conclusions

In this study, to achieve high transparency, the fully dense transparent spinel body was fabricated by the rapid and efficient SPS method. LiF nano powder (0.7 wt %) was synthesized chemically at different temperatures and concentrations on the spinel particles surface to prepare the RSS powder. Also, the RSS powder was synthesized with a homogenous distribution of LiF nano powder at the temperature of 60

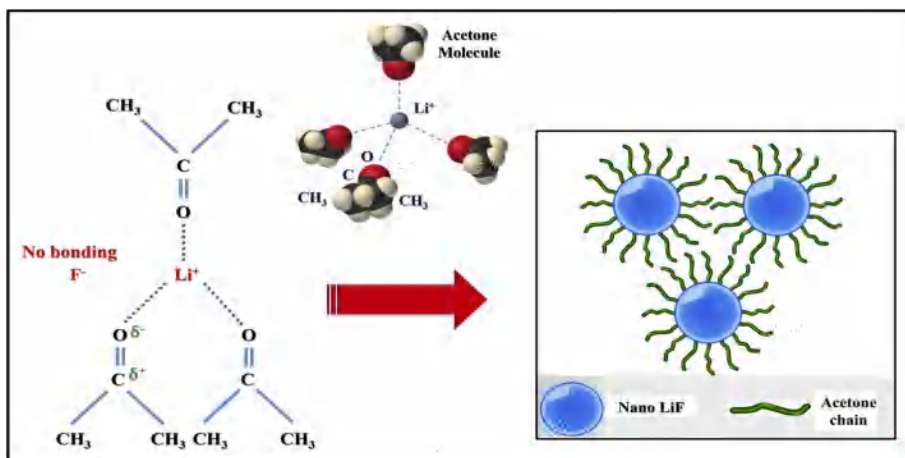


Fig. 10. The schematic of in-situ chemical synthesis in the presence of acetone and LiF solvation effect.

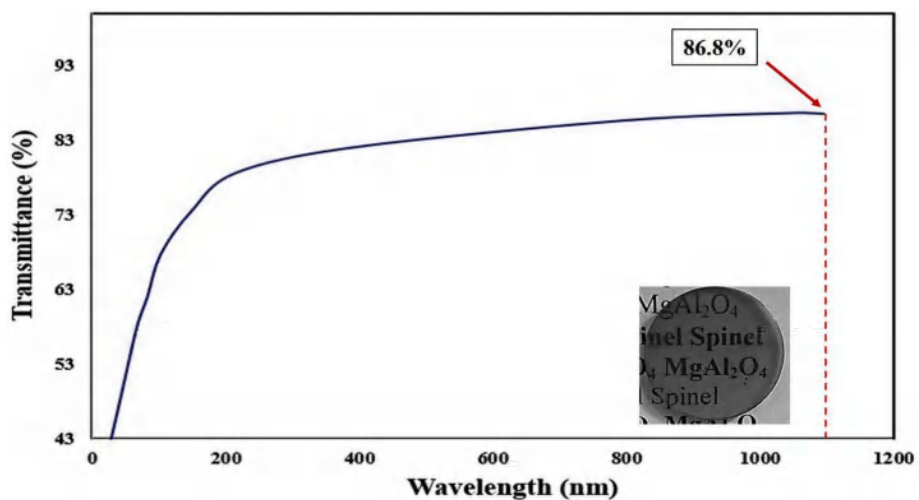


Fig. 11. The in-line transmittance diagram of the SPS-sintered RSS powder.

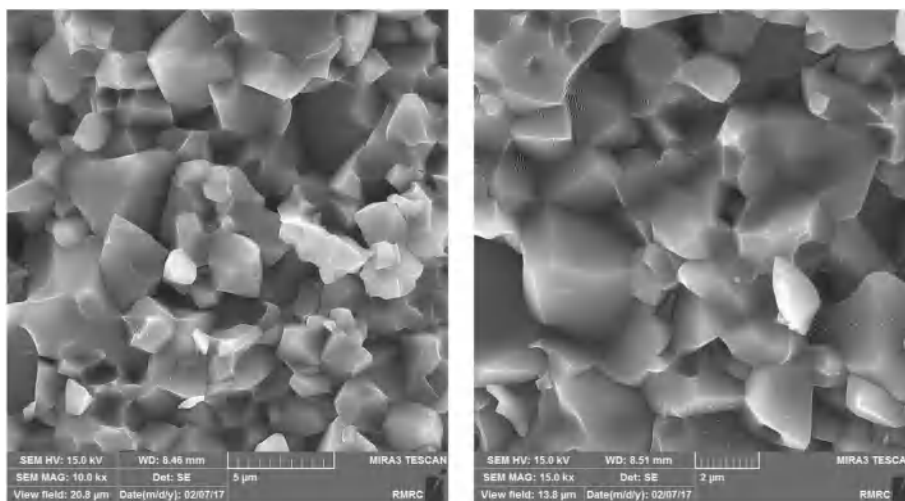


Fig. 12. The fracture surface of the sintered body.

°C, with the concentration of 200 g/l LiOH solution and the addition of acetone. The results of TEM (HAADF detector), FE-SEM (EDS detector) and XRD also demonstrated the presence of the fluoride light element (LiF compound) on the spinel particles surface. After sintering at 1100 °C, the final strength, density, and transmission at the wavelength of 1100 nm of the spinel body were measured 97.8 MPa, 99.98%, and 86.8%, respectively.

Declaration of competing interest

The authors declare that they have no known competing financial interests or personal relationships that could have appeared to influence the work reported in this paper.

Appendix A. Supplementary data

Supplementary data to this article can be found online at <https://doi.org/10.1016/j.matchemphys.2020.123035>.

References

- [1] Y. Liu, J. Zhu, Fabrication of transparent MgAl_2O_4 ceramics by gelcasting and cold isostatic pressing, *Ceram. Int.* 46 (2020) 4154–4158.
- [2] T. Kato, D. Nakauchi, N. Kawaguchi, T. Yanagida, Optical, scintillation, and dosimetric properties of dy-doped MgAl_2O_4 transparent ceramics, *Optik (Stuttg.)* 207 (2020), 164433.
- [3] G. Kerbart, C. Harnois, C. Bilot, S. Marinel, Pressure-assisted microwave sintering: a rapid process to sinter submicron sized grained MgAl_2O_4 transparent ceramics, *J. Eur. Ceram. Soc.* 39 (2019) 2946–2951.
- [4] S. Takahashi, A. Kan, H. Ogawa, Microwave dielectric properties and crystal structures of spinel-structured MgAl_2O_4 ceramics synthesized by a molten-salt method, *J. Eur. Ceram. Soc.* 37 (2017) 1001–1006.
- [5] S.K. Mohan, R. Sarkar, Effect of ZrO_2 addition on MgAl_2O_4 spinel from commercial grade oxide reactants, *Ceram. Int.* 42 (2016) 10355–10365.
- [6] P. Biswas, A. Sharma, M. Krishnan, R. Johnson, M.K. Mohan, Fabrication of MgAl_2O_4 spinel scaffolds and sonochemical synthesis and deposition of hydroxyapatite nanorods, *J. Am. Ceram. Soc.* 99 (2016) 1544–1549.
- [7] S.K. Mohan, Densification and Characterization of Magnesium Aluminate Spinel from Commercial Grade Reactants: Effect of Milling and Additives, 2016.
- [8] J. Rufner, D. Anderson, K. Benthem, R.H.R. Castro, Synthesis and sintering behavior of ultrafine (< 10 nm) magnesium aluminate spinel nanoparticles, *J. Am. Ceram. Soc.* 96 (2013) 2077–2085.
- [9] S.F. Wang, J. Zhang, D.W. Luo, F. Gu, D.Y. Tang, Z.L. Dong, G.E.B. Tan, W.X. Que, T.S. Zhang, S. Li, Transparent ceramics: processing, materials and applications, *Prog. Solid State Chem.* 41 (2013) 20–54.
- [10] I. Ganesh, A review on magnesium aluminate (MgAl_2O_4) spinel: synthesis, processing and applications, *Int. Mater. Rev.* 58 (2013) 63–112.
- [11] H. Shahbazi, M. Tataei, M.H. Enayati, A novel technique of gel-casting for producing dense ceramics of spinel (MgAl_2O_4), *Ceram. Int.* 45 (2019) 8733.
- [12] K. Morita, B.-N. Kim, K. Hiraga, H. Yoshida, Fabrication of transparent MgAl_2O_4 spinel polycrystal by spark plasma sintering processing, *Scr. Mater.* 58 (2008) 1114–1117.
- [13] K. Waetzig, T. Hutzler, Highest UV–vis transparency of MgAl_2O_4 spinel ceramics prepared by hot pressing with LiF, *J. Eur. Ceram. Soc.* 37 (2017) 2259–2263.
- [14] J. Liu, X. Lv, J. Li, L. Zhang, J. Peng, Densification and microstructure of magnesium aluminate spinel for adding method of Sc_2O_3 , *J. Alloys Compd.* 735 (2018) 394–399.
- [15] M. Han, Z. Wang, Y. Xu, R. Wu, S. Jiao, Y. Chen, S. Feng, Physical properties of MgAl_2O_4 , CoAl_2O_4 , NiAl_2O_4 , CuAl_2O_4 , and ZnAl_2O_4 spinels synthesized by a solution combustion method, *Mater. Chem. Phys.* 215 (2018) 251–258.
- [16] M. Shamim, S. Sinhamahapatra, J. Hossain, S. Lahiri, K. Dana, Kinetic analysis of magnesium aluminate spinel formation: effect of $\text{MgO}:\text{Al}_2\text{O}_3$ ratio and titania dopant, *Ceram. Int.* 44 (2018) 1868–1874.
- [17] S. Sanjabi, A. Obeydavi, Synthesis and characterization of nanocrystalline MgAl_2O_4 spinel via modified sol–gel method, *J. Alloys Compd.* 645 (2015) 535–540.
- [18] S. Sahoo, Study on the Effect of the Effect of Different Raw Materials Sources on Spinelization and Densification of $\text{MgO}:\text{Al}_2\text{O}_3$ Spinel, 2014.
- [19] J.F. Rufner, R.H.R. Castro, T.B. Holland, K. van Benthem, Mechanical properties of individual MgAl_2O_4 agglomerates and their effects on densification, *Acta Mater.* 69 (2014) 187–195.
- [20] H. Shahbazi, M. Tataei, M.H. Enayati, A. Shafeiey, M.A. Malekabadi, Structure-transmittance relationship in transparent ceramics, *J. Alloys Compd.* 785 (2019) 260–285.
- [21] Y. Zou, D. He, X. Wei, R. Yu, T. Lu, X. Chang, S. Wang, L. Lei, Nanosintering mechanism of MgAl_2O_4 transparent ceramics under high pressure, *Mater. Chem. Phys.* 123 (2010) 529–533.
- [22] H. Shahbazi, H. Shokrollahi, M. Tataei, Gel-casting of transparent magnesium aluminate spinel ceramics fabricated by spark plasma sintering (SPS), *Ceram. Int.* 44 (2018) 4955–4960.
- [23] H. Shahbazi, H. Shokrollahi, A. Albaji, Optimizing the gel-casting parameters in synthesis of MgAl_2O_4 spinel, *J. Alloys Compd.* 712 (2017) 732–741.
- [24] H. Shahbazi, M. Tataei, Influence of porosity on transparency behavior of MgAl_2O_4 spinel, experiment vs Mie theory, *Opt. Mater. (Amst.)* 90 (2019) 289–299.
- [25] D.S. Suarez, E.G. Pinna, G.D. Rosales, M.H. Rodriguez, Synthesis of lithium fluoride from spent lithium ion batteries, *Minerals* 7 (2017) 81.
- [26] Y. Sun, H.-W. Lee, G. Zheng, Z.W. Seh, J. Sun, Y. Li, Y. Cui, In situ chemical synthesis of lithium fluoride/metal nanocomposite for high capacity prelithiation of cathodes, *Nano Lett.* 16 (2016) 1497–1501.
- [27] F. Nikanjam, R. Sarraf-Mamoory, N. Riahi-Noori, Optimizing parameters in synthesis of LiF nanopowders via sol–gel method, *Nano* 6 (2011) 575–581.
- [28] C. Wall, A. Pohl, M. Knapp, H. Hahn, M. Fichtner, Production of nanocrystalline lithium fluoride by planetary ball-milling, *Powder Technol.* 264 (2014) 409–417.
- [29] S.K. Mohan, R. Sarkar, A comparative study on the effect of different additives on the formation and densification of magnesium aluminate spinel, *Ceram. Int.* 42 (2016) 13932–13943.
- [30] S. Meir, S. Kalabukhov, N. Froumin, M.P. Dariel, N. Frage, Synthesis and densification of transparent magnesium aluminate spinel by SPS processing, *J. Am. Ceram. Soc.* 92 (2009) 358–364.
- [31] R. Marder, R. Chaim, G. Chevallier, C. Estournès, Effect of 1 wt% LiF additive on the densification of nanocrystalline Y_2O_3 ceramics by spark plasma sintering, *J. Eur. Ceram. Soc.* 31 (2011) 1057–1066.
- [32] A.C. Sutorik, G. Gilde, C. Cooper, J. Wright, C. Hilton, The effect of varied amounts of LiF sintering aid on the transparency of alumina rich spinel ceramic with the composition $\text{MgO}_{-1.5}\text{Al}_2\text{O}_3$, *J. Am. Ceram. Soc.* 95 (2012) 1807–1810.
- [33] W. Luo, R. Xie, M. Ivanov, Y. Pan, H. Kou, J. Li, Effects of LiF on the microstructure and optical properties of hot-pressed MgAl_2O_4 ceramics, *Ceram. Int.* 43 (2017) 6891–6897.
- [34] K.G. Rozenburg, An Investigation on the Role of Lithium Fluoride in the Sintering of Magnesium Aluminate Spinel, 2009.
- [35] A. Katz, E. Barraud, S. Lemonnier, E. Sorrel, M. Eichhorn, S. d’Astorg, A. Leriche, Role of LiF additive on spark plasma sintered transparent YAG ceramics, *Ceram. Int.* 43 (2017) 15626–15634.
- [36] L. Esposito, A. Piancastelli, S. Martelli, Production and characterization of transparent MgAl_2O_4 prepared by hot pressing, *J. Eur. Ceram. Soc.* 33 (2013) 737–747.
- [37] K. Rozenburg, I.E. Reimanis, H. Kleebe, R.L. Cook, Sintering kinetics of a MgAl_2O_4 spinel doped with LiF, *J. Am. Ceram. Soc.* 91 (2008) 444–450.
- [38] L. Esposito, A. Piancastelli, P. Miceli, S. Martelli, A thermodynamic approach to obtaining transparent spinel (MgAl_2O_4) by hot pressing, *J. Eur. Ceram. Soc.* 35 (2015) 651–661.
- [39] K. Rozenburg, I.E. Reimanis, H. Kleebe, R.L. Cook, Chemical interaction between LiF and MgAl_2O_4 spinel during sintering, *J. Am. Ceram. Soc.* 90 (2007) 2038–2042.
- [40] A. Shafeiey, M.H. Enayati, A. Albaji, The effect of slip casting and spark plasma sintering (SPS) temperature on the transparency of MgAl_2O_4 spinel, *Ceram. Int.* 44 (2018) 3536–3540.
- [41] N. Frage, S. Cohen, S. Meir, S. Kalabukhov, M.P. Dariel, Spark plasma sintering (SPS) of transparent magnesium-aluminate spinel, *J. Mater. Sci.* 42 (2007) 3273–3275.
- [42] A. Zegadi, M. Kolli, M. Hamidouche, G. Fantozzi, Transparent MgAl_2O_4 spinel fabricated by spark plasma sintering from commercial powders, *Ceram. Int.* 44 (2018) 18828–18835.
- [43] M.A. Malekabadi, R.S. Mamoory, Low-temperature synthesis of micro/nano Lithium Fluoride added magnesium aluminate spinel, *Ceram. Int.* 44 (2018) 20122–20131.
- [44] M.T. Vu, Densification and Characterization of Transparent Polycrystalline Spinel Produced by Spark Plasma Sintering, 2014.
- [45] R.O. Loutfy, J.L. Sepulveda, S. Chang, Ready-to-sinter Spinel Nanomixture and Method for Preparing Same, 2012.
- [46] R. Sarraf-Mamoory, S. Naderi, N. Riahi-Noori, The effect of precipitation parameters on preparation of lithium fluoride (LiF) nano-powder, *Chem. Eng. Commun.* 194 (2007) 1022–1028.
- [47] G.R. Villalobos, J.S. Sanghera, S.S. Bayya, I.D. Aggarwal, Magnesium Aluminate Transparent Ceramic Having Low Scattering and Absorption Loss, 2011.
- [48] G.R. Villalobos, J.S. Sanghera, S.S. Bayya, I.D. Aggarwal, Spinel and Process for Making Same, 2009.
- [49] G.R. Villalobos, J.S. Sanghera, S. Bayya, I.D. Aggarwal, Fluoride Salt Coated Magnesium Aluminate, 2007.
- [50] G.R. Villalobos, J.S. Sanghera, W. Kim, S.S. Bayya, B. Sadowski, I.D. Aggarwal, Sintering Aid Coated YAG Powders and Agglomerates and Methods for Making, 2016.
- [51] G. Villalobos, S. Bayya, W. Kim, C. Baker, J. Sanghera, M. Hunt, B. Sadowski, F. Miklos, I. Aggarwal, Low absorption magnesium aluminate spinel windows for high energy laser applications, *J. Mater. Res.* 29 (2014) 2266–2271.
- [52] G.R. Villalobos, J.S. Sanghera, S. Bayya, I.D. Aggarwal, Method for Fluoride Salt Coated Magnesium Aluminate, 2009.
- [53] G.R. Villalobos, J.S. Sanghera, S. Bayya, I.D. Aggarwal, W. Kim, B. Sadowski, LiF-coated Doped and Undoped Yttrium Oxide, 2008.
- [54] P. Fu, W. Lu, W. Lei, Y. Xu, X. Wang, J. Wu, Transparent polycrystalline MgAl_2O_4 ceramic fabricated by spark plasma sintering: microwave dielectric and optical properties, *Ceram. Int.* 39 (2013) 2481–2487.
- [55] S. Benaissa, M. Hamidouche, M. Kolli, G. Bonnefont, G. Fantozzi, Characterization of nanostructured MgAl_2O_4 ceramics fabricated by spark plasma sintering, *Ceram. Int.* 42 (2016) 8839–8846.